SUPRAMOLECULAR POLYMERS

EDITED BY

ALBERTO CIFERRI

University of Genoa
Genoa, Italy

Duke University
Durham, North Carolina

MARCEL DEKKER, INC. NEW YORK • BASEL

10

Self-Assembled Monolayers (SAMs) and Synthesis of Planar Micro- and Nanostructures

Lin Yan
Bristol-Myers Squibb, Princeton, New Jersey

Wilhelm T. S. Huck and George M. Whitesides
Harvard University, Cambridge, Massachusetts

I. INTRODUCTION: SAMs AS TWO-DIMENSIONAL POLYMERS

A polymer, by conventional definition, is a macromolecule made up of multiple equivalents of one or more monomers linked together by *covalent bonds* (e.g., carbon–carbon, amide, ester, or ether bonds) [1]. These conventional polymers come in many configurations: for example, linear homopolymers, linear copolymers, block copolymers, crosslinked polymers, dendritic polymers, and others. The most common architecture for polymers is based on linear chains that may have other attached chains (branched, grafted, or crosslinked); that is, they are one-dimensional molecules. A few examples have been claimed as two-dimensional sheet polymers.*

A supramolecular polymer is a structure in which monomers are organized through *noncovalent interactions* (e.g., hydrogen bonds, electrostatic interactions, and van der Waals interactions) [4]. These less familiar types of polymers also exist in many forms. For example, molecular crystals are large collections of molecules arranged in a three-dimensional periodical lattice through noncovalent

* See Refs. 2 and 3 and references therein.

intermolecular interactions. Lipid bilayers are two-dimensional structures that exist in water, in which hydrocarbon tails aggregate to form a hydrophobic sheet in the form of a spherical shell, and polar or charged hydrophilic head-groups are exposed to water.

Self-assembled monolayers (SAMs) are highly ordered molecular assemblies that form spontaneously by chemisorption of functionalized molecules on surfaces, and organize themselves laterally, most commonly by van der Waals interactions between monomers [5]. We consider SAMs to be a type of two-dimensional polymer: they are, in a sense, a uniform supramolecular assembly of short hydrocarbon chains covalently grafted onto a macromolecular entity, that is, the surface. In SAMs, individual monomers (usually linear alkyl chains functionalized at one end or both) are not directly linked by covalent bonds to each other, but rather to a common substrate—a metal or a metal oxide surface. SAMs exist in a number of different types: homogeneous SAMs on planar and curved substrates, SAMs on metallic liquids, SAMs on nanoparticles, mixed SAMs, and two-dimensionally patterned SAMs. Table 1 compares some characteristics of SAMs and conventional polymers based on bonding and structural type.

Table 1 Comparison Between Conventional Polymers and SAMs, Considered as Two-Dimensional Polymers

		Conventional polymers	SAMs
Nature of bonding	Short range	Covalent bonding between adjacent monomers	Covalent bonding between head-groups and the substrate; van der Waals, H-bonding, ionic interactions between adjacent monomers
	Long range	van der Waals, H-bonding, ionic interactions between monomeric units proximate in space	No
Structural types		Homopolymers Copolymers (alternating, block, and random) Linear, branched, cross-linked, dendrimeric, etc.	Homogeneous SAMs Mixed SAMs Patterned SAMs
Conformational class		Extended Collapsed Random coiled	Crystalline Disordered Liquidlike

Figure 1 describes the formation of these two types of polymers schematically. A conventional linear polymer is formed by polymerization that links monomers through chemical reactions (e.g., free radical, ionic, and coordination addition, condensation, and ring opening reactions). Polymer chains are often conformationally disordered: in dilute solution, polymer chains are often coiled; in concentrated solution or in bulk, they are entangled. For SAMs, ''polymerization'' is a spontaneous process involving adsorption that connects monomers to a substrate, and self-organization that orders the system laterally through noncovalent intermolecular interactions. The strong chemical interaction between the head-group and the substrate renders the ''shape'' of a SAM two-dimensional, and its ''size'' the surface area of the substrate. The overall structure of SAMs is determined by the interaction of the head-group and the substrate, the lateral interaction between the neighboring monomers, and the structure of the constituent monomers. SAMs supported on metals or metallic oxides are not soluble, and thus provide no information about the behavior of two-dimensional soluble polymers. They are, however, excellent models for the surface chemistry of insoluble polymers, and among the motivations for the study of SAMs are to understand the physical-organic chemistry of polymer surfaces [6–8], and to develop

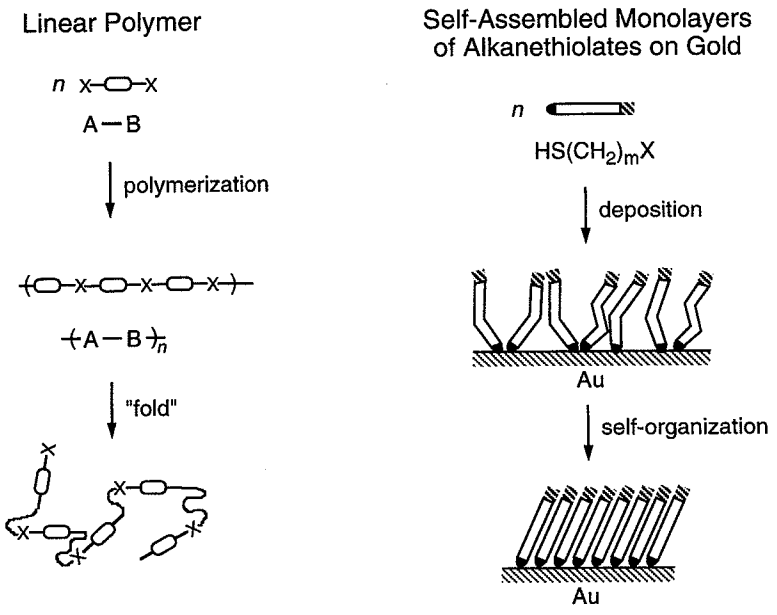

Figure 1 Schematic representation of the formation of conventional polymers and of self-assembled monolayers (SAMs).

methods that can be used to control interfacial properties of polymers at the molecular level [9].

This chapter considers SAMs as two-dimensional polymers, and describes the synthesis and structures of SAMs comprising one thiol, and mixed SAMs and patterned SAMs comprising more than one thiol (mainly on gold and silver). It reviews some recent studies of chemical transformations of terminal functional groups of SAMs after their assembly, and discusses two potentially useful chemical methods developed in our group for synthesis of mixed SAMs and patterned SAMs, and several of their applications.

II. SYSTEMS OF SAMs

The monomeric units of conventional polymers can be connected by different kinds of chemical bonds; correspondingly SAMs can have various chemical inter-

Table 2 Different Types of SAMs ($CH_3(CH_2)_nX$)

Head group (X)	Precursor	SAMs of	Substrate	Bonding
RS	RSH or $RS)_2$	Alkanethiolates	Au[14], Ag[15], Cu[16], Pd[29], Fe, Fe_2O_3[30], Hg[31], GaAs[32,33], InP[34]	$RS^-{\cdot}M_n^{+n}$ or $RS)_2$; M^n
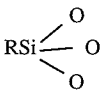	$RSiCl_3$, $RSi(OCH_3)_3$, or $RSi(OEt)_3$	Alkylsiloxanes	SiO_2, glass, mica[23,25], Al_2O_3[35], $Ga_2{}^{37}O_3{}^{32}$, Au[36,37]	Polymeric siloxane
RA^-	RCO_2H	Acid-functionalized alkanes	Al_2O_3[35,38–42], In_2O_3/SnO_2[43], SiO_2[41], AgO, CuO[40]	Acid-base
	RCONHOH		Au, Al_2O_3, ZrO_2, Fe_2O_3, TiO_2, AgO, CuO[44]	
	RSO_2H		Au[45]	
	RPO_3H_2		SiO_2, ZrO_2, Al_2O_3, TiO_2, mica[46–48]	
RB	R_2S, R_3P	Base-functionalized alkanes	Au[49–52]	Coordination
	RNC		Au[53], Pt[50]	
R	RCH_3	Alkyl groups	Si, graphite [54–56]	Covalent Si-C

actions between the head-group and the supporting substrate. A number of different types of SAMs have been explored; several of these systems have been reviewed [5,10–13]. Table 2 categorizes SAMs into groups based on the bonding between the head-group and the surface. The most widely studied systems have been SAMs formed by chemisorption of alkanethiols on gold [14], silver [15], or copper [16]. SAMs of phosphonates have been widely used to synthesize multilayer structures with application in nonlinear optic devices [17–19] and heterogeneous catalysis [18,19]. SAMs of siloxanes on glass and metallic oxides have been studied by Sagiv [22,23] and others [24–27], and widely used technologically in surface treatment [28]. SAMs covalently attached to these substrates provide a rugged system for various applications, but certain of these systems—especially those based on $-SiCl_3$ or $-Si(OEt)_3$ head-groups—can be difficult to synthesize, and the reactivity of these head-groups may be incompatible with other functional groups.

SAMs of alkanethiolates that present a wide range of functional groups on thin polycrystalline films of gold and silver are easy to prepare, and have been broadly applied in various fundamental and technological studies. They are well ordered, and the best characterized systems of organic monolayers presently known. In this chapter, we focus on them.

III. SYNTHESIS OF SAMs ON GOLD AND SILVER

The preparation of SAMs of alkanethiolates on gold and silver is straightforward. The metal substrates are prepared by evaporation of a thin layer of titanium or chromium (~1–5 nm; this layer of Ti or Cr promotes the adhesion of gold or silver to the supporting substrate) onto silica wafers, glass slides, or other flat surfaces, followed by deposition of gold or silver (~10–200 nm; in general, ≥40 nm is required to achieve a complete coverage of the substrate) [57]. SAMs of alkanethiolates (e.g., $X(CH_2)_nSH$, X is a terminal functional group) on gold and silver can be easily generated by immersing the metal substrate in 1–10 mM solutions of alkanethiols at room temperature; ethanol is commonly used as the solvent [Eq. (1)]; SAMs can also be generated using vapor phase deposition [58] or electrodeposition [59] of alkanethiols.

$$X(CH_2)_nSH + Au(0)_m \rightarrow X(CH_2)_nS^-Au(I) \cdot Au(0)_{m-1} + \frac{1}{2H_2} \quad (1)$$

Although formation of SAMs on gold is usually expressed as Eq. (1), the mechanistic details of this reaction remain incompletely understood. It is generally believed that the thiol group forms a thiolate ($RS^-Au(I)$) in its interaction with gold [13]. Some studies using grazing-angle X-ray diffraction have, how-

ever, been interpreted to suggest that the interaction of sulfur and gold involves a disulfide ($R_2S_2Au(0)$) [60]. Using molecular dynamics (MD), Gerdy and Goodard have calculated a hypothetical crystal structure for decyl disulfide on Au(111) surface, and found that the resulting structure was energetically stable and the X-ray diffraction pattern derived from such structure was indistinguishable from that observed experimentally [61]. Most of the theoretical studies have, however, been based on the assumption of interactions of thiolates and gold [62]. A conclusive description about the interaction between the sulfur and gold awaits additional experimental and theoretical studies [63]. The fate of the hydrogen atom of the thiol group has also not been resolved. Although there remain a number of uncertainties concerning the structure of the interface between SAMs and gold, most of the interest in SAMs has focused on the structure of the polymethylene $(CH_2)_n$ groups, and on the interaction of the tail groups with the solution; it is thus immaterial, to some extent, what the binding is between gold and surface.

The kinetics of formation of SAMs on gold has been studied using a range of methods: ellipsometry [64], contact angle [64], quartz crystal microbalance (QCM) [65–69], surface acoustic wave (SAW) [70], surface plasmon resonance (SPR) [71], optical second harmonic generation (SHG) [72], polarized infrared external reflectance spectroscopy (PIERS) [73], scattering Raman spectroscopy [74], and electrochemistry [75]. These studies provide a macroscopic picture of the processes that form SAMs: the growth rate is proportional to the number of unoccupied sites on gold, and can be described as a first-order Langmuir adsorption. Recent atomic force microscopy (AFM) [76] and scanning tunneling microscopy (STM) [77–79] studies depict a three-stage microscopic process:

1. Lattice gas phase—alkanethiols are confined on the surface and diffuse rapidly.
2. Low-density solid phase—molecular axes are aligned with the surface plane and the close pairing of thiol groups is maintained.
3. High-density pseudocrystalline solid phase—alkanethiols are closely packed and their axes are aligned with the surface normal.

Synthesis of SAMs is remarkably convenient: it requires only ambient conditions, and the substrate can be polycrystalline or even electroless gold and silver films [80,81]. Formation of SAMs of a single alkanethiol on gold is known to complete in a few minutes, and may occur in seconds during microcontact printing (μCP), a process in micropatterning [82,83]. SAMs on gold are one of the systems of SAMs most widely used.

IV. STRUCTURES OF SAMs ON GOLD AND SILVER

The molecular structures of SAMs have been studied extensively using various instrumental techniques: PIERS [84–87], X-ray photoelectron spectroscopy

(XPS) [64,88], AFM [89–91], grazing-angle X-ray diffraction [92], molecule beam diffraction [93,94], high-energy electron scattering [95], low-energy electron diffraction [57], electrochemistry [96,97], ellipsometry [85,98], and contact angle [87,98–100]. The packing of alkanethiolates on gold is influenced by the spacing of coordination sites and the interaction between the adjacent alkyl chains. Electron diffraction and low-energy helium beam diffraction studies suggest that the sulfur atoms are localized in threefold hollow sites of the Au(111) surface and form a commensurate triangular $\sqrt{3} \times \sqrt{3}R30°$ overlayer lattice (Fig. 2) [57,95,101]. In a SAM of *n*-alkanethiolates, the average cross-sectional area occupied by each thiolate is 21.4 $Å^2$; this value is larger than that of an alkane chain (18.4 $Å^2$). The alkyl chains adopt a largely *trans* conformation (for $n \geq 10$) and tilt ~30° with respect to the surface normal in order to maximize van der Waals interactions between adjacent polymethylene chains (the enthalpy of lateral interaction per CH_2 group is ~1.5 kcal/mol). Although the distance between nearest silver atoms (2.89 Å) on the Ag(111) surface is similar to that of gold (2.88 Å), in SAMs of alkanethiolates on silver, the sulfur atoms arrange themselves in a $\sqrt{7} \times \sqrt{7}R10.9°$ lattice and the alkyl chains are nearly perpendicu-

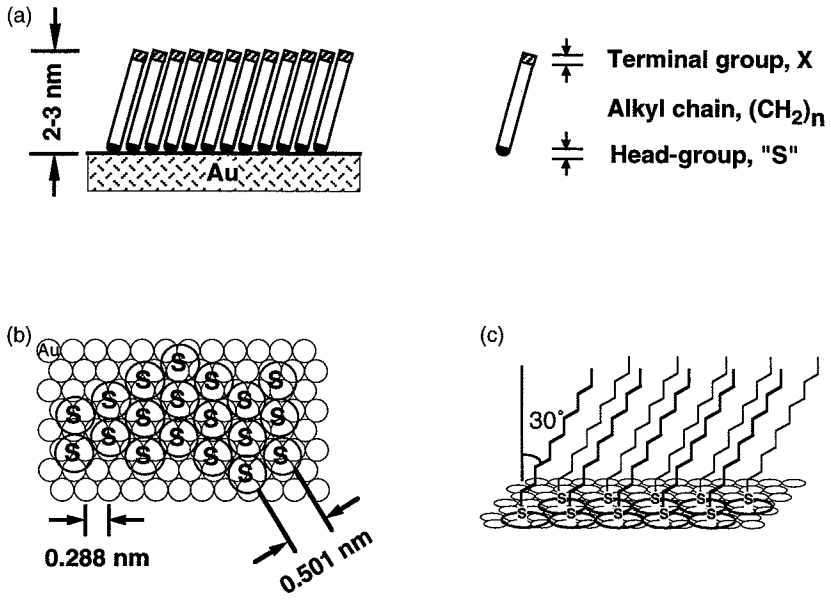

Figure 2 (a) A schematic representation of SAMs of *n*-alkanethiolates on gold. (b) The $\sqrt{3} \times \sqrt{3}R30°$ lattice of sulfur atoms on Au(111). (c) Alkyl chains adopt all *trans* conformation and tilt ~30° from the normal of the surface.

lar to the surface (tilt ~10° from the normal of the substrate) [102]. Using ab initio calculations, Ulman and coworkers suggest that the combination of the lateral discrimination of chemisorption potentials and unfavorable charge–charge interactions between both the thiolates and the underlying Au atoms in SAMs prevent the alkyl chains from packing as densely as those on silver [103]. SAMs formed on freshly prepared silver substrates generally have a lower population of gauche conformations than SAMs on gold, but silver is readily oxidized by oxygen in air and a thick film of silver oxide does not support a well-ordered SAM of alkanethiolates. In general, SAMs of alkanethiolates on freshly prepared silver should be considered more highly ordered than analogous structures on gold.

Although experimental studies have sketched a structural picture of SAMs on gold and silver, the details of this picture remain incompletely defined: among the remaining uncertainties are the exact position of sulfur atoms on gold, the bond angle of the metal-S-C group, the nature of the interaction of the chains with one another, and the nature of lateral movement. Theoretical studies can, in principle, contribute to understanding these issues, although SAMs represent very complex systems for computation. Most of the theoretical work has been carried out on SAMs on gold [62]. Ulman and coworkers have used a very simple model to simulate the thickness of the film, and the molecular orientation and packing of alkyl chains on gold [104]. To a first approximation, they first optimized the geometry of isolated molecules, and then constructed small hexagonal assemblies of these rigid molecules. Considering only van der Waals and electrostatic intermolecular interactions, they examined the interaction energy of a molecule with its neighbor as a function of tilt angles, and found that the calculated thickness and the tilt angles were the same as those established from experimental studies. Klein and coworkers have used MD to investigate the structure and dynamics of alkanethiols on gold [105–108]. They first pinned all the alkyl chains perpendicularly onto a well-defined triangular lattice with the nearest neighbor distance of 4.97 Å and then allowed the system to relax and to evolve into energetically minimal structures. Using both the united-atom model and the more realistic all-atom model, they found that most of the alkyl chains adopted *trans* conformations, and that the system had fewer gauche conformations when the metal-S-C bonds are colinear than 90°. They also found that the average conformation was temperature-dependent: SAMs were less ordered at high temperature, which observation agreed with the results derived from molecular beam studies. Siepmann and coworkers have used Monte Carlo (MC) methods to study the properties of SAMs on gold [109]. Grunze and coworkers have used stochastic global search to explore the configurational space of a SAM of octadecanethiol, $CH_3(CH_2)_{17}SH$, on gold [110]. They used four different force fields and found that several distinct monolayer structures could exist with energy difference less than 1 kcal/mol. Using ab initio calculation, Ulman and coworkers found that thiolates prefer the threefold hollow sites over the on-top sites, but Bishop and

coworkers used MD and found that the energy difference within the surface corrugation potential is too small to pin sulfur atoms at any particular site [111].

The order of the terminal group and the top part of SAMs is determined not only by the sulfur atoms bound directly to the gold and the intermolecular interaction between the alkyl chains, but also by the size and geometry of the terminal group. STM studies show that SAMs of alkanethiolates on gold are heterogeneous and structurally complex. The alkyl chains form a ''superlattice'' at the surface of the monolayer of sulfur atoms, that is, a lattice with symmetry and dimensions different from that of the underlying hexagonal lattice formed by sulfur atoms. When alkanethiolates are terminated with end-groups other than the methyl group, the structure of the resulting SAM becomes less predictable. Nelles and coworkers have shown that the superlattice is dependent on the shape of the terminal groups: thiols having terminal groups with relatively spherical cross-sections form hexagonal lattices; thiols with more asymmetric cross-sections form centered rectangular lattices [112]. Sprik and coworkers have used STM and MD to study SAMs terminated with hydrophilic groups such as hydroxyl and amine groups, and found hydrogen bond induced reconstruction of the top layer and coadsorption of solvents [113].

For SAMs of thiols having tail groups more complicated than *n*-alkyl chains, the structures of SAMs depend on the size and geometry of these groups. Tao and others have shown that thiols derivatized with aromatic groups form well-ordered SAMs having a packing order different from *n*-alkanethiolates: the sulfur atoms form a $\sqrt{3} \times \sqrt{3}R30°$ lattice on gold, but the aromatic groups adopt a herringbone packing and are perpendicular to the surface [114–118]. SAMs of fluorinated alkanethiolates also pack differently [119,120]. The fluorinated alkyl groups have a van der Waals diameter of 5.6 Å (i.e., larger than that of the 5.0 Å diameter of normal alkyl groups). They form a 2×2 lattice and tilt $\sim 16°$ from the normal of surface.

Although SAMs are self-assembling systems and tend to reject defects, the presence of defects and pinholes is always observed [121–123]. A variety of factors influences formation and distribution of defects in a SAM, including the molecular structure of the surface, the length of the alkyl chain, and the conditions used to prepare SAMs. Grunze and coworkers have recently described a procedure in which a SAM of alkanethiolates on gold is treated with mercury vapor, then exposed again to a solution of alkanethiol. This procedure seems to heal defects in the SAM by increasing the density of alkyl chains and causing them to reorient to a tilt angle from the normal that resembles that characteristic of copper and silver [124].

V. FUNCTIONAL AND MIXED SAMs ON GOLD

SAMs presenting a variety of functional groups have been applied in a broad range of fundamental studies; representative areas include biocompatibility [125],

wetting [126], adhesion [126,127], corrosion [14,128,129], and micro- and nanofabrication [130]. The strong chemo-specific interaction between the thiol group and gold (~24–40 kcal/mol) [12] gives SAMs high stability under mild conditions (room temperature) and allows SAMs to display a wide range of organic functionalities in high density ($\sim 2 \times 10^{14}$ molecules/cm^2) on the surface. Van der Waals interactions between adjacent polymethylene chains force alkanethiolates to pack at densities approaching those of crystalline poly(ethylene); these lateral interactions make SAMs impermeable to molecules in solution [131–134], and give them the electrical insulating properties similar to that of poly(ethylene) [135]. These characteristics allow the chemical and physical properties of the terminal functional groups that are exposed on the surface largely to determine the interfacial properties of a SAM. For example, oligo(ethylene glycol) and oligo(propylene sulfoxide) groups presented on SAMs of undecanethiolates on gold shelter the hydrophobic underlying polymethylene chains effectively from contacting proteins in solution and thus provide a surface that resists nonspecific adsorption of proteins [136–138]. These studies demonstrate that functional SAMs provide well-defined model systems to study surface phenomena.

SAMs that present a mixture of different functional groups–''mixed'' SAMs—provide desirable flexibility in design and synthesis of functional SAMs

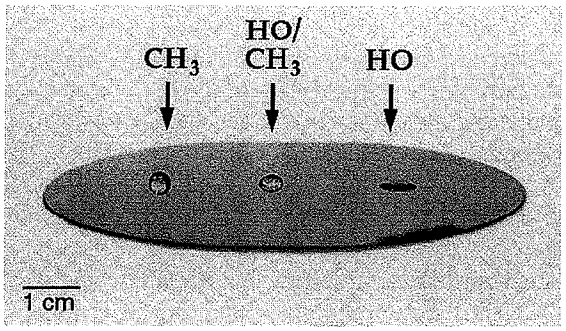

Figure 3 On this 4-inch gold-coated silicon wafer, three different kinds of SAMs were formed. The left part was covered with a SAM of $HS(CH_2)_{15}CH_3$ (a hydrophobic surface), the right part with a SAM of $HS(CH_2)_{11}OH$ (a hydrophilic surface), and the middle area with a mixed SAM of $HS(CH_2)_{15}CH_3$ and $HS(CH_2)_{11}OH$ (formed from a solution containing the two in a ~1:1 ratio). A droplet of water was placed on each of these regions. The shape of the droplet on the mixed SAM was intermediate between that on the hydrophobic and hydrophilic surfaces. This simple experiment shows that the terminal groups on the SAM can control interfacial properties (here, wetting) and also demonstrates the capability of mixed SAMs to tailor the surface properties by controlling the ratio of mixed functionalities on the surface.

that span a wider range of chemical and physical properties than do pure SAMs [21,139]. It becomes straightforward to tune continuously the interfacial properties of a SAM simply by varying the ratio of compositions of two thiols in the mixed SAM. Synthesis of mixed SAMs on gold is convenient: the gold-coated substrate is immersed in a solution containing two different thiols at a certain ratio, usually for 8 h; the resulting SAM contains a mixture of these two alkyl groups. Figure 3 shows the influence of a terminal group of SAMs on the shape of a droplet of water that contacts the surface. The wetting of water on the surface of a SAM having a ~1:1 mixture of HS $(CH_2)_{15}CH_3$ and $HS(CH_2)_{11}OH$ is intermediate between that of a SAM having $HS(CH_2)_{15}CH_3$ and that having a SAM of $HS(CH_2)_{11}OH$. The ratio of two components in the SAM is often different from that in solution [139]. Although the two organic groups of a mixed SAM are often well-mixed [140], thiols that have different properties can phase-separate into domains having only one type of thiols; whether this separation is kinetic or thermodynamic is not known [139,141]. AFM and STM studies show that the size of these phase-separated domains is ~50 nm [142–144]. The microscopic heterogeneity does not influence many of the macroscopic chemical and physical properties of the SAMs.

VI. CHEMICAL REACTIONS ON SAMs AFTER THEIR ASSEMBLY

Chemical transformation of terminal functional groups of SAMs *after* their assembly has recently attracted attention. There are several reasons to study chemical reactions on SAMs. They provide (i) controllable well-defined model systems with which to understand the influence of a surface on chemical reactions of functional groups; (ii) alternative methods to functionalize SAMs, to construct multilayers, and to attach molecules and biomolecules to surfaces; (iii) a possible basis for strategies for synthesis of combinatorial libraries of small molecules on a chip; and (iv) synthetic model systems that can be extended to chemical functionalization of polymer surfaces.

A variety of terminal functional groups and their chemical transformations on SAMs have been examined: for example, (i) olefins—oxidation [23,24,131,132], hydroboration, and halogenation [23,24]; (ii) amines—silylation [145,146], coupling with carboxylic acids [22,146], and condensation with aldehydes [22,147]; (iii) hydroxyl groups—reactions with anhydrides [148,149], isocyanates [150], epichlorohydrin [151], and chlorosilanes [152]; (iv) carboxylic acids—formation of acyl chlorides [153], mixed anhydrides [154], and activated esters [148,155]; (v) carboxylic esters—reduction and hydrolysis [156]; (vi) thiols and sulfides—oxidation to generate disulfides [157–159] and sulfoxides [160]; and (vii) aldehydes—condensation with active amines [161]. Nucleophilic

displacement on SAMs has also been investigated mainly on SAMs of alkylsiloxanes on Si/SiO_2 [146,162–164]. These studies have shown that many organic reactions that work well in solution are difficult to apply to transformations at the surface, because the surface is a sterically hindered environment, and backside reactions (e.g., the S_N2 reaction) and reactions with large transition states (e.g., esterification, saponification, Diels–Alder reaction, and others) often proceed slowly. At present, only few synthetic methods are used, but those are capable of introducing a wide range of functional groups onto the surface.

The difficulty of developing useful chemical transformations on the surface is substantially compounded by lack of efficient techniques to identify products and to establish their yields after each reaction. PIERS and XPS are two particularly useful methods to characterize chemical transformations on the surface. PIERS provides direct evidence of transformation of an infrared-active functional group; XPS furnishes evidence for the presence or absence of an element characteristic of the functional group being introduced or eliminated, and is often used to estimate qualitatively the yield of chemical transformation. Other methods, such as ellipsometry, contact angle, secondary ion mass spectroscopy (SIMS) [165], and AFM [166] also provide complementary and valuable support for characterization of chemical reactions on SAMs. Establishing unambiguously the products and yield of a chemical reaction on the surface often requires a combination of information from several techniques.

We have developed two convenient chemical methods that may have general utility for rapid synthesis of functional SAMs. The first procedure has three steps (Fig. 4) [167]: preparation of a well-ordered homogeneous SAM of 16-mercaptohexadecanoic acid on gold; conversion of the terminal carboxylic acid groups into interchain carboxylic anhydrides by reaction with trifluoroacetic anhydride; and reaction of the interchain carboxylic anhydride with an alkylamine to give a mixed SAM presenting carboxylic acids and *N*-alkyl amides on its surface. Figure 5 summarizes the characterization of the product of transformation of terminal carboxylic acids to interchain carboxylic anhydrides, and of anhydrides to a $\sim 1:1$ mixture of acids and amides. SAMs of 16-mercaptohexadecanoic acid show C=O stretches at 1744 and 1720 cm^{-1} that are characteristic of terminal carboxylic acid groups presented on a SAM [87]. Treatment of the SAM with trifluoroacetic anhydride gives a SAM having C=O stretches at 1826 and 1752 cm^{-1}; these frequencies are characteristic of a carboxylic anhydride group [168]. XPS studies of the resulting SAM show no fluorine. The combination of these results indicates that the carboxylic acid group is converted into an interchain carboxylic anhydride group by trifluoroacetic anhydride, rather than to a mixed trifluoroacetic carboxylic anhydride. After reaction of the interchain carboxylic anhydride with *n*-undecylamine (taken as a representative *n*-alkylamine), the C=O stretches of the anhydride disappear completely, and two new absorption bands appear at 1742 and 1563 cm^{-1}; these bands are assigned as the C=O stretch of a carboxylic acid and an amide II band, respectively. XPS also

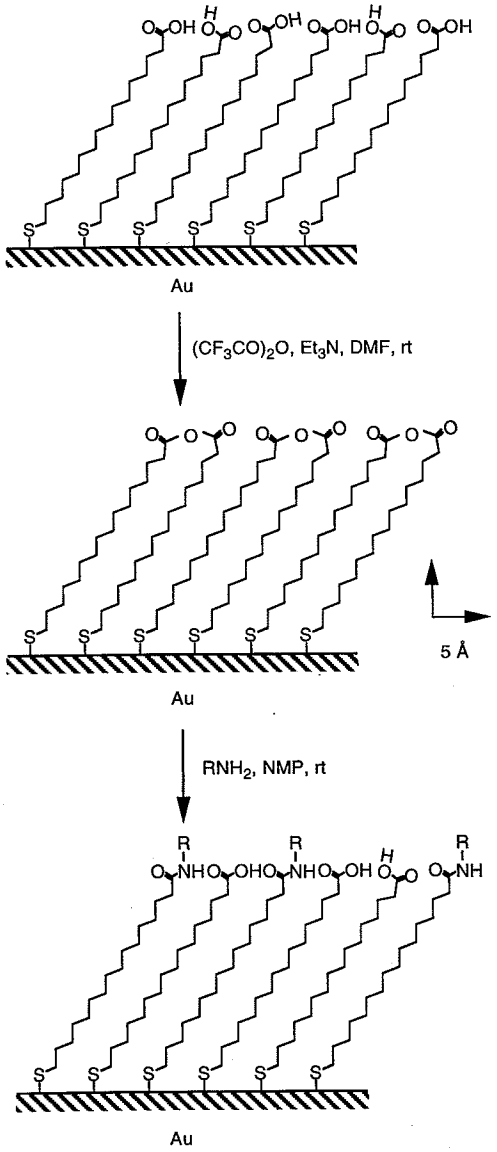

Figure 4 Schematic representation of formation of the interchain carboxylic anhydride and reaction of the anhydride with an alkylamine. The alkyl chains of the original SAM of the carboxylic acid in these SAMs are in *trans* conformation; the methylene groups near the functional groups may adopt gauche conformation and be less ordered. Carboxylic acids in the SAMs of the carboxylic acid, and in the mixed SAMs of amides and carboxylic acids, are hydrogen bonded to neighboring polar groups. The interchain carboxylic anhydrides orient largely parallel to the surface normal. (From Ref. 167.)

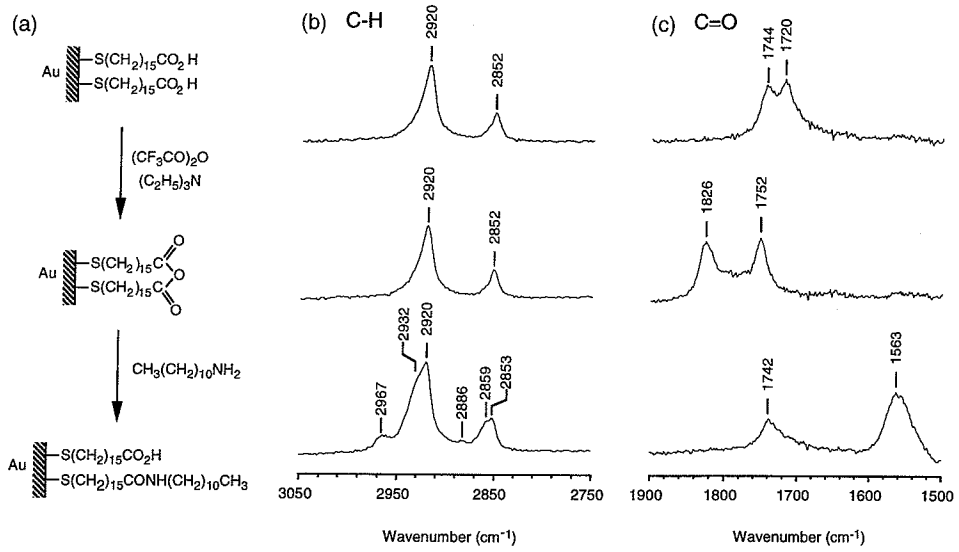

Figure 5 Comparison of PIERS spectra of the SAMs of the carboxylic acid, the interchain carboxylic anhydride, and a mixture of carboxylic acids and *n*-undecylamides on gold: (a) schematic representation of formation of the interchain carboxylic anhydride and the reaction of the anhydride and *n*-undecylamine; (b) the PIERS spectra of these SAMs in the C—H stretching region; (c) the PIERS spectra of these SAMs in the C=O stretching region. (From Ref. 167.)

indicates the presence of nitrogen in the resulting sample. The combination of these results suggests the coupling of amines to the SAM. PIERS further shows that there are two low-frequency shoulder peaks at 2932 and 2859 cm^{-1} in the resulting sample, which are the methylene stretches of the *n*-undecyl chain; these peak positions suggest that the alkyl chains of the original SAM remain in a *trans* conformation, but that the new alkyl chains are disordered and contain more gauche conformations [167]. These transformations on the surface occur rapidly, and in close to quantitative yield. This new chemical method using interchain carboxylic anhydride as a reactive intermediate has allowed for rapid introduction of many functionalities into SAMs, for example, *n*-alkyl groups [167], perfluorinated *n*-alkyl groups [169], peptides [170], charged groups (sulfonate and guanidine groups) [169], and polymers containing amine groups [e.g., poly(ethylene imine)] [171]; all that is required is a molecule containing that functionality and also an active amine group. This method provides access to SAMs that can be inconvenient or impossible to prepare using the older methods.

Figure 6 compares the second method—the common intermediate method—with the older but more commonly used method. This method also has

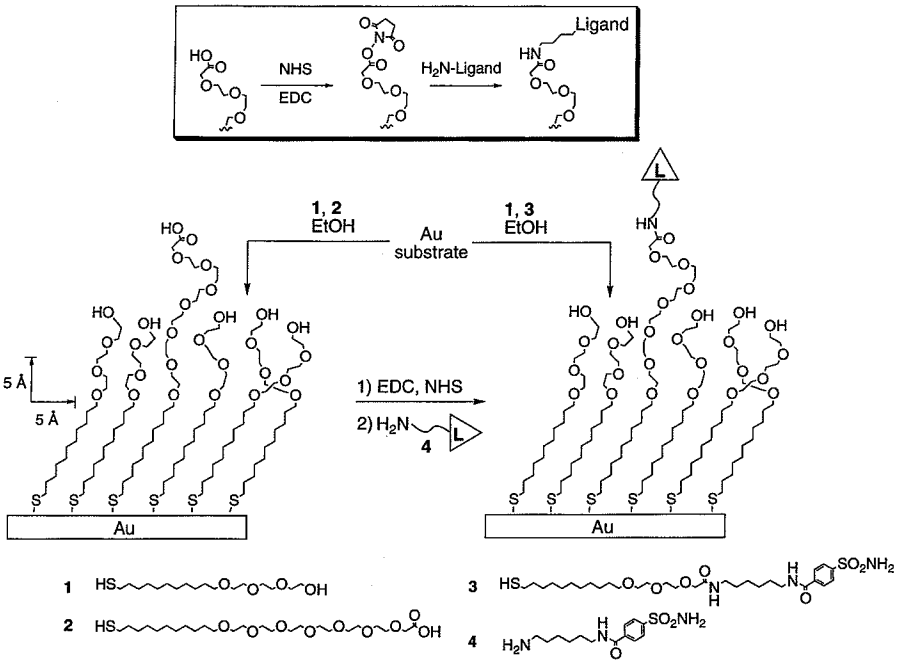

Figure 6 Schematic comparison of the common intermediate method and the older method involving the synthesis of ligand-terminated alkanethiols for preparation of SAMs presenting ligands. In the common intermediate method, a SAM bearing carboxylic acid groups is formed by immersing gold substrates in a mixture of alkanethiols **1** and **2**. This mixed SAM, after activation with NHS and EDC, presents an active NHS ester group on the surface that serves as a common intermediate for the attachment of different ligands by amide bond formation. The upper panel illustrates the chemical transformations involving carboxylic acid groups: (i) activation of carboxylic acid groups with NHS and EDC to generate active NHS esters, and (ii) displacement of the NHS group with an amino group on the ligand (a benzenesulfonamide-containing amine **4** as a representative ligand) or ϵ-amino groups of lysine residues of proteins to form an amide bond. The polymethylene chains of the alkanethiols in the SAMs are drawn in all-*trans* conformation; this conformation has been observed in SAMs of long chain alkanethiols on gold. The oligo(ethylene glycol) groups are depicted with little or no ordering; the detailed conformation in these SAMs has not been firmly established. (From Ref. 172.)

three steps [172]: formation of a mixed SAM of alkanethiolates on gold derived from the tri(ethylene glycol) ($(EG)_3OH$) terminated thiol ($HS(CH_2)_{11}(OCH_2CH_2)_3OH$; **1**) and the hexa(ethylene glycol)-carboxylic acid ($(EG)_6CO_2H$) terminated thiol ($HS(CH_2)_{11}(OCH_2CH_2)_6OCH_2CO_2H$; **2**); generation of activated *N*-hydroxylsuccinimidyl (NHS) esters of thiol **2**; and reaction with proteins, peptides, or small molecules containing active amine groups. These reactions are characterized using PIERS and ellipsometry. Figure 7 shows the PIERS spectra of SAMs of **1**, of **2**, of an authentic thiol ($HS(CH_2)_{11}(OCH_2CH_2)_6OCH_2CONH(CH_2)_6NHCOC_6H_4SO_2NH_2$; **3**), of a mixed SAM comprising **1** and **2**, and of the products of the subsequent reactions. Upon treatment of the mixed SAM

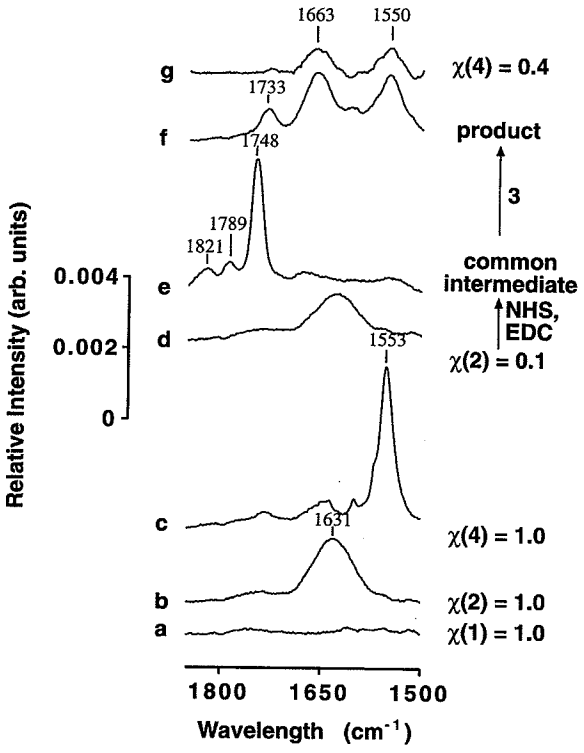

Figure 7 PIERS data for: (i) a homogeneous SAM of **1**; (ii) a homogeneous SAM of **2**; (iii) a homogeneous SAM of **3**; (iv) a mixed SAM comprising **1** and **2** with $\chi(2) = 0.10$; (v) a mixed SAM comprising **1** and **2** with $\chi(2) = 0.10$ after activation with NHS and EDC in H_2O; (vi) a mixed SAM comprising **1** and **2** with $\chi(2) = 0.10$ after treatment with NHS and EDC followed by reaction with **4**; and (vii) a mixed SAM comprising **1** and **3** with $\chi(3) = 0.40$. (From Ref. 172.)

with *N*-hydroxylsuccinimide (NHS) and 1-ethyl-3-(3-dimethylaminopropyl)carbodiimide (EDC), the appearance of bands diagnostic for the NHS ester at 1789 cm^{-1} (symmetric stretch of imide C=O groups) and 1821 cm^{-1} (C=O stretch of the activated ester carbonyl group) indicates the formation of active NHS ester groups on the surface. The complete disappearance of the band at 1631 cm^{-1}, which is assigned as the C=O stretch of a carboxylic acid, suggests near quantitative conversion of carboxylic acid groups to NHS esters. After treatment with a benzenesulfonamide-containing amine ($NH_2(CH_2)_6NHCOC_6H_4SO_2NH_2$; **4**), PIERS shows the appearance of bands at 1550 and 1660 cm^{-1} (characteristic of N—H bending modes) and a weak band at 1733 cm^{-1} (C=O stretch of carboxylic acid groups). Comparison by PIERS with an authentic SAM of **3** established that benzenesulfonamide ligands were covalently attached to the mixed SAM through amide bonds. Bovine carbonic anhydrase II (CA) can recognize and reversibly bind to the immobilized benzenesulfonamide ligand on the surface [172]. We have also used this procedure to attach proteins to SAMs [172].

VII. PATTERNING OF SAMs ON GOLD IN THE PLANE OF THE MONOLAYER

Patterning SAMs in the plane of the monolayer is useful in determining the two-dimensional distribution of chemical and physical properties on a surface. There are several methods available for generation of patterned SAMs. Microcontact printing is a convenient technique that "stamps" a pattern of SAM directly on a surface (Fig. 8) [82,83]. In μCP, an elastomeric poly(dimethylsiloxane) (PDMS) stamp—fabricated by casting and curing PDMS against masters that present patterned photoresist on silicon wafers—is wetted or inked with an alkanethiol and brought into contact with the gold-coated substrate; SAMs form on the areas that contacted the stamp. SAMs presenting different functional groups can be subsequently formed on the uncontacted areas, either by μCP or by immersion in a solution of another thiol. The edge resolution of the patterns resulting from μCP is ~50 nm [173]. AFM studies show that the structural order characterizing alkanethiolates in SAMs formed by μCP is the same as that deriving from immersion of the gold substrate in a solution of thiol [174]. μCP offers a convenient, low cost, flexible, and nonphotolithographic method to pattern SAMs on large areas [175] and curved substrates [176], and also to pattern SAMs of other systems: alkanethiolates on coinage metals [134], alkylsiloxanes on Si/SiO_2 and glass [177,178], and colloids [179,180] and proteins on various substrates [181,182].

Combination of μCP and chemical reaction on a reactive SAM, for example, a SAM presenting interchain carboxylic anhydride groups, can simplify and extend μCP [169]. Figure 9 shows an example: a PDMS stamp with protruding

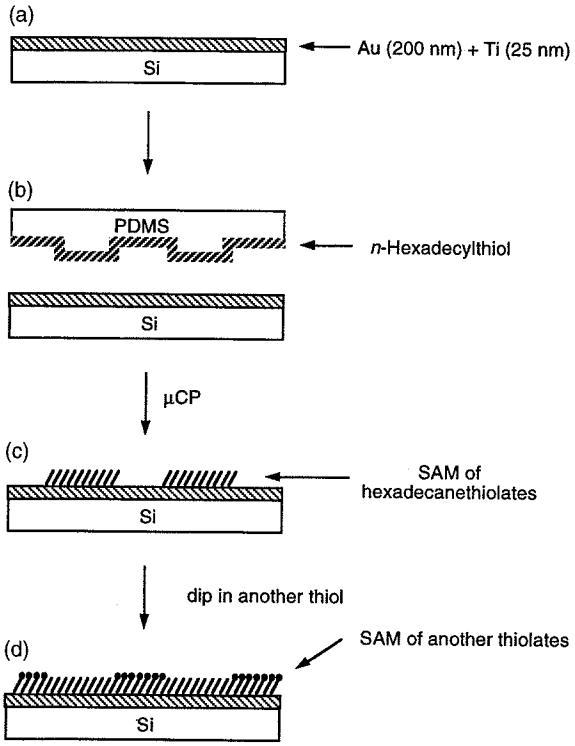

Figure 8 Schematic illustration for μCP of *n*-hexadecanethiol on gold followed by dipping into a solution containing another thiol.

features (squares having ~10 μm on a side) prints *n*-hexadecylamine on the reactive SAM to give a SAM comprising a~1:1 mixture of *N*-alkyl amides and carboxylic acids. The remaining anhydride groups in the uncontacted regions are allowed to react with another amine, $CF_3(CF_2)_6CH_2NH_2$ to give a patterned SAM having regions presenting *N*-hexadecyl amides and fluorinated *N*-alkyl amides. SEM images (Fig. 10) indicate that the edge resolution of these squares is at submicron scale (≤100 nm). The high contrast and uniformity in the SEM and SIMS images (Fig. 10) suggest that μCP delivered a well-defined pattern of *n*-hexadecylamine to the reactive SAM on both gold and silver. The key chemical reaction—the reaction of amine and surface anhydride—proceeds rapidly and in close to quantitative yield under ambient experimental conditions, with good edge

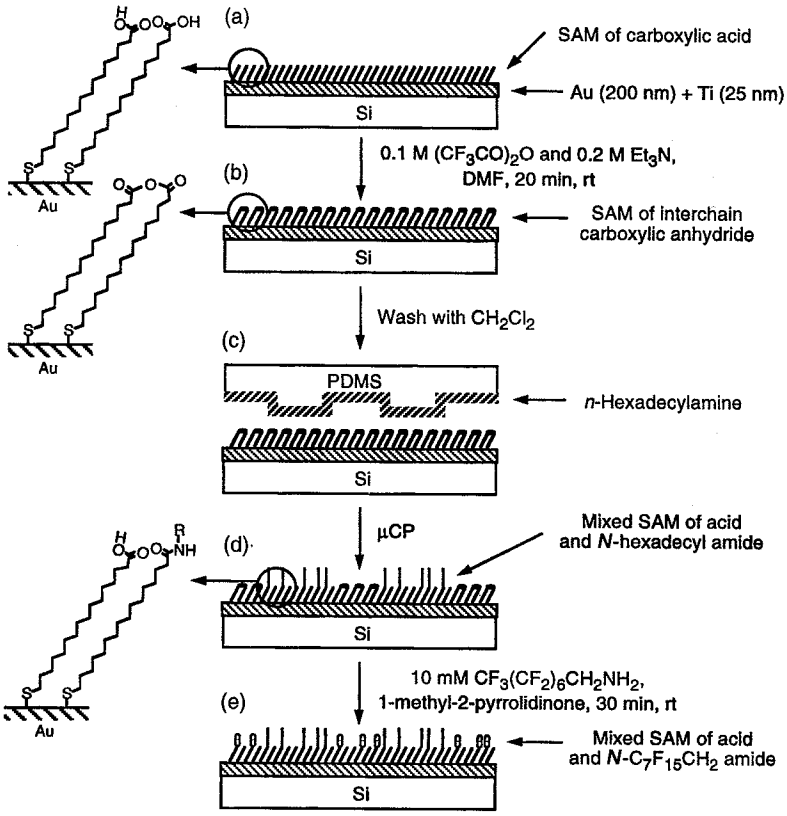

Figure 9 Schematic outline of the procedure for patterning a SAM that presents two different *N*-alkyl amides using μCP and a chemical reaction. The diagram represents the composition of the SAM but not the conformation of the groups in it. (From Ref. 169.)

definition. This method provides a straightforward route to patterned SAMs that present a variety of functional groups.

VIII. APPLICATIONS

SAMs of alkanethiolates on gold provide excellent model systems for studies on interfacial phenomena (e.g., wetting, adhesion, lubrication, corrosion, nucleation, protein adsorption, cell attachment, and sensing). These subjects have been re-

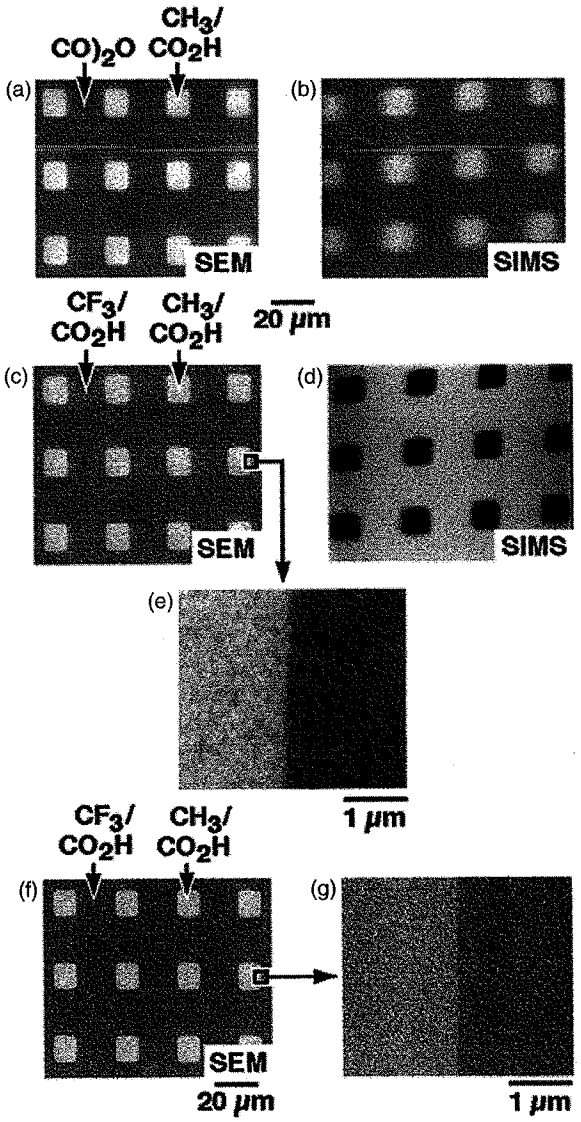

Figure 10 Characterization using SEM and SIMS of the patterned SAMs on Au (a)–(e) and on Ag (f) and (g) generated by μCP of *n*-hexadecylamine on the reactive SAM followed by reaction with $CF_3(CF_2)_6CH_2NH_2$. The light areas in the SEM images were the regions contacted by the stamp. The light squares in SIMS image (b) contained nitrogen while the dark regions did not; the light regions in SIMS image (d) had fluorine while the dark squares did not. The patterns in the SIMS images were distorted because the sample holder was slightly tilted during acquisition of these images. (From Ref. 169.)

viewed previously [125,183–185]. Here we focus on applications that involve using chemical synthesis of functional SAMs after their assembly.

A. Patterning Thin Films of Polymer

Patterned thin films of polymers have many applications e.g., in preventing etching [177], in molecular electronics [186–188], in optical devices [189,190], in biological [191] and chemical sensors [154,192], and in tissue engineering [193]. Thin films of polymers that have reactive functional groups present a surface that can be further modified by chemical reactions [194,195]. There are several methods available for attaching polymers to SAMs: electrostatic adsorption of polyelectrolytes to an oppositely charged surface [196,197], chemisorption of polymers containing reactive groups to a surface [198,199], and covalent attachment of polymers to reactive SAMs [151,154,200,201]. There are presently only a few methods available for patterning thin films of polymers on SAMs; these include procedures based on photolithography [200,201], templating the deposition of polymers using patterned SAMs [197,202,203], and templating phase-separation in diblock copolymers [204,205]. Patterned thin films of polymers attached covalently to the surface are more stable than are ones only physically adsorbed. Photochemical pattern transfer offers only limited control over the surface chemistry, the properties, and the structure of the modified surfaces.

Combination of μCP and chemical modification of the reactive SAM presenting interchain carboxylic anhydride groups provides a convenient method for patterning thin films of amine-containing polymers having submicron-scale edge resolution on the surface [171]. Figure 11 describes this approach. A reactive SAM presenting interchain carboxylic anhydride groups is prepared using trifluoroacetic anhydride (Fig. 4). A PDMS stamp with protruding squares (~10 μm on a side) on its surface is oxidized for ~10 sec with an oxygen plasma. The oxidized PDMS stamp is immediately inked with a 1 wt% solution of poly(ethylene imine) (PEI) in 2-propanol and placed in contact with the substrate. The anhydride groups in the regions that contacted the PDMS stamp react with the amine groups of PEI. Removal of the stamp and hydrolysis of the remaining anhydride groups with aqueous base (pH = 10, 5 min) give a surface patterned with PEI. All these procedures are carried out under ambient conditions; the entire process—from the readily available SAMs of 16-mercaptohexadecanoic acid to the final patterned PEI films—can be completed in less than one hour.

The AFM images acquired in contact mode show that μCP delivered a well-defined pattern of PEI to the reactive SAM (Fig. 12). The resulting thin films of PEI are nearly continuous, but their surfaces are not smooth at the nanometer scale (Fig. 12b). The roughness of these films is controlled in part by the surface topology of the polycrystalline gold substrate, and probably also by the presence of gel or dust particles in the PEI. Line analysis indicates that the aver-

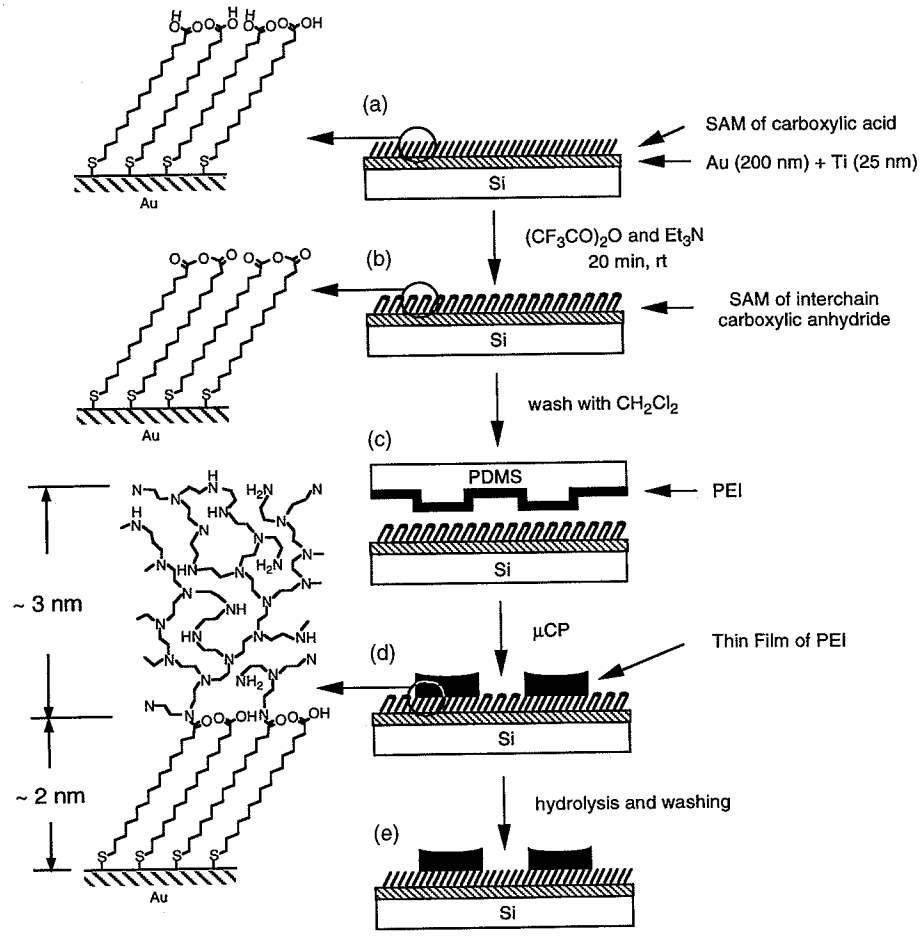

Figure 11 Schematic description of the procedure for patterning thin films of PEI on the surface of a SAM using μCP and a chemical reaction. The scheme suggests the composition of the SAM, but not the conformation of the groups in it; it also makes no attempt to represent either the conformation of the polymer or the distribution of functional groups on the polymer backbone.

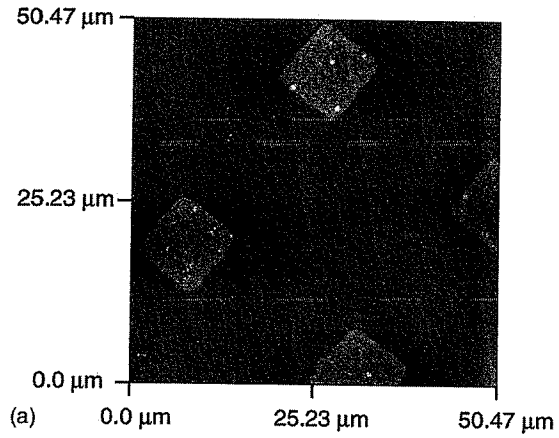

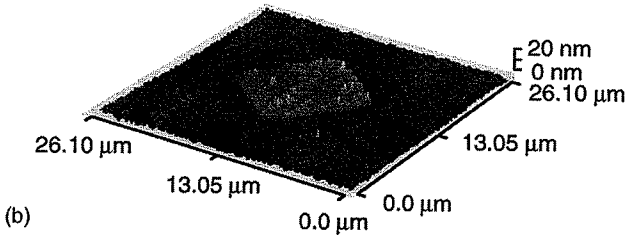

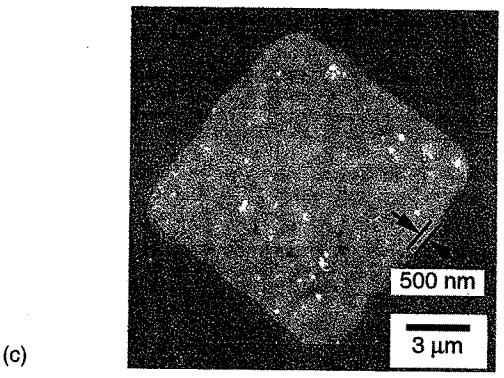

Figure 12 Contact mode AFM characterized the patterned thin films of PEI generated by μCP of PEI on the reactive SAM; these images show a sample patterned by μCP, followed by hydrolysis of the remaining, unreacted interchain carboxylic anhydrides with aqueous base. The light squares in the AFM images (a)–(c) were thin films of PEI on the regions contacted by the PDMS stamp. The AFM image (c) shows that the PEI film was separated by a well-defined boundary (with roughness <500 nm) from the regions presenting carboxylic acid groups. The lines in the images were artifacts generated by the instrument. (From Ref. 171.)

age thickness of the patterned thin films is ~3 nm. Figure 12c suggests that the edge resolution of these squares is at the submicron scale (<500 nm); this value is larger than that obtained in μCP of *n*-hexadecylamine on the reactive SAM (<100 nm) and of alkanethiolates on gold (<50 nm). Because PEI is a hydrophilic polymer, it is essential to make the hydrophobic PDMS stamp hydrophilic using oxygen plasma prior to inking in order to form continuous, patterned thin films of PEI on the surface [206]. PIERS studies further show that PEI is covalently linked to the SAM by amide bonds and that the PEI films are thus more stable under both acidic and basic conditions than are polymers physically adsorbed on SAMs of carboxylic acids.

The covalently attached PEI films make a large number of reactive amine groups available for further chemical modification of the surface. These amine groups can react with other functional groups (e.g., acyl chlorides and carboxylic anhydrides) to introduce different organic functionalities into the surface, and to attach polymers that have such organic functional groups. We have shown that the amine groups of the attached PEI film can react with perfluorooctanoyl chloride, palmitoyl chloride, palmitic anhydride, and poly(styrene-*alt*-maleic anhydride) [171].

B. Facile Preparation of SAMs That Present Mercaptan, Charged, and Polar Groups

Chemical reaction provides a straightforward method for the preparation of SAMs that present a variety of functional groups—especially polar, charged, or structurally complex groups, such as peptides, polymers, and oligosaccharides—that are difficult to prepare using deposition of thiols terminated at these groups [169].

Figure 13 shows a patterned SAM presenting methyl and thiol groups, and the subsequent assembly of Au nanoparticles in the regions presenting thiol groups. The patterned SAM is generated by μCP of *n*-hexadecylamine on the reactive SAM followed by reaction with cysteamine ($HSCH_2CH_2NH_2$). Patterned SAMs presenting thiol groups are difficult to prepare by conventional μCP. The resulting patterned substrate is then immersed in an aqueous suspension of Au nanoparticles stabilized with citrate anions. SEM images show that the Au nanoparticles assemble predominately in the thiol-presenting regions, and the width of the border separating the region having adsorbed nanoparticles from that having none is <100 nm.

We have prepared SAMs presenting sulfonates and guanidines by allowing the reactive SAM to react with 3-amino-1-propanesulfonic acid ($H_2N(CH_2)_3SO_3H$) and agmatine sulfate ($H_2N(CH_2)_4NHC(=NH)NH_2 \cdot H_2SO_4$). For the SAM presenting sulfonates, XPS shows a signal at 168.5 eV; we assign this peak to S(2p) of a sulfonate, and the advancing and receding contact angles

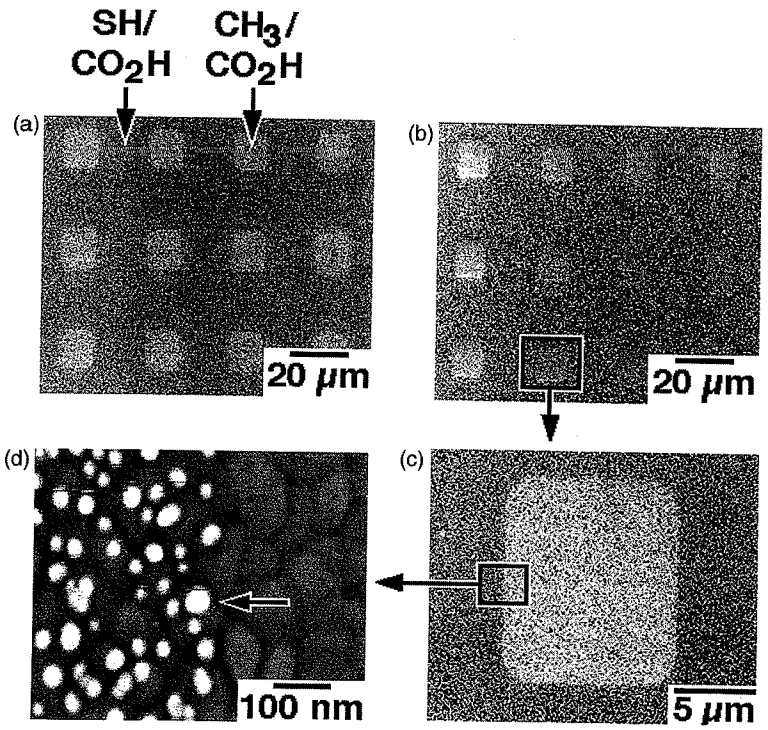

Figure 13 SEM images of (a) a patterned SAM presenting methyl groups (white squares) and thiol groups; (b), (c), and (d) patterned deposition of Au nanoparticles (white dots pointed by an arrow in (d) in the regions that present thiol groups. The background texture in (d) is the "islands" that are formed on evaporating gold under the conditions we used. The mean diameter of the Au nanoparticles was ~20 nm. (From Ref. 169.)

of water are both less than 10° (the lowest value we can measure). For the SAM presenting guanidines, XPS shows an N(1 s) signal at 400.4 eV, the advancing contact angle of water is 47°, and the receding contact angle 30°.

C. Wetting

Previous extensive studies of carboxylic acid functionalized poly(ethylene) films (PE—CO_2H) [207–209], of SAMs terminated in ionizable acids and bases [100], of mixed SAMs of carboxylic acid- and methyl-terminated alkanethiolates [210], and of SAMs of dialkyl sulfides on gold [211] have established the utility of contact angle titration in characterizing the wetting properties of interfaces. We

have determined the advancing contact angle of water θ_a as a function of pH for several mixed monolayers obtained by allowing the interchain anhydride to react with homologous *n*-alkylamines (*n*-$C_nH_{2n+1}NH_2$, n = 0, 1, 4, 6, 11, and 18) (Fig. 14). In these mixed SAMs, the polar carboxylic acid groups are buried beneath hydrocarbon layers of different thickness.

The values of θ_a for the SAMs derivatized with long *n*-alkylamines (n = 11 and 18) do not change with pH. These alkyl groups form thick hydrophobic films (ca. 10 and 15 Å, respectively) that prevent water from contacting the buried carboxylic acid groups. The values of θ_a change with pH for mixed SAMs derivatized with short *n*-alkylamines (n = 1, 4, and 6). There are significant features of these data. First, the titration curves do not reach a plateau at high pH; the same behavior is observed for the mixed SAMs of carboxylic acid- and methyl-terminated alkanethiolates on gold prepared from mixtures of $HS(CH_2)_{10}COOH$ and $HS(CH_2)_{10}CH_3$ [211]. By contrast, the carboxylic acid functionalized material obtained by oxidizing poly(ethylene) (PE—CO_2H) does achieve plateau values at high pH [207]. Second, the onset points of ionization are approximately pH

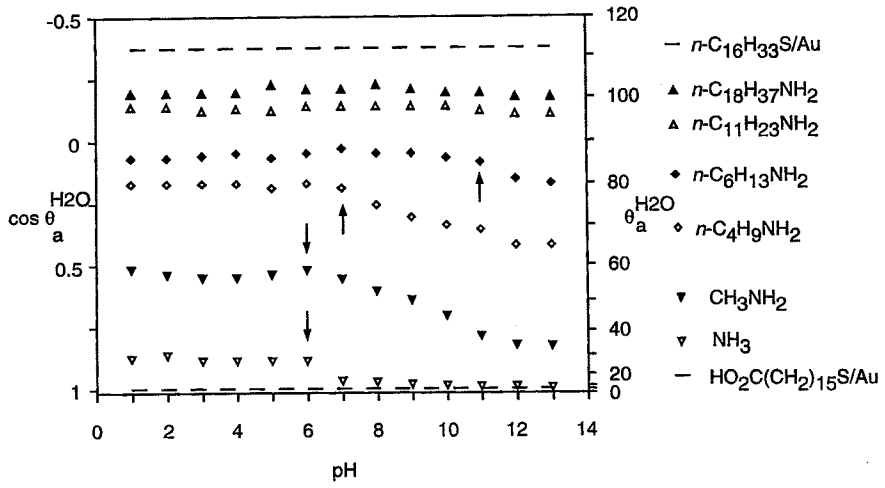

Figure 14 Dependence of the advancing contact angle (θ_a) of buffered aqueous solutions of different values of pH on the SAMs comprising a mixture of carboxylic acids and amides, generated by reactions of the interchain anhydride and alkylamines (*n*-$C_nH_{2n+1}NH_2$, n = 0, 1, 4, 6, 11, and 18). The curves are labeled by the respective alkylamines on the right side of the plot. Two dashed lines on the top and the bottom of the plot are reference data for θ_a of $CH_3(CH_2)_{15}S/Au$ and $HO_2C(CH_2)_{15}S/Au$, respectively, as indicated. Arrows indicate the onset points of ionization of carboxylic acid groups.

11 for the *n*-hexylamine-modified SAM and approximately pH 7 for the *n*-butylamine-modified SAM. The values of θ_a also change with pH for mixed SAMs comprising carboxylic acids and *N*-methyl amide and primary amides. These titration curves are very similar to that of the mixed SAM of *N*-butyl amides and carboxylic acids. Both the onset points of ionization are approximately at pH 6. Such shifts from the values expected on the basis of titration in aqueous solution are similar to those observed with mixed SAMs terminated with carboxylic acid and methyl groups [211].

Contact angle titrations of these *n*-alkylamine-modified SAMs suggest that these systems are more like mixed SAMs of methyl- and carboxylic acid-terminated alkanethiolates on gold than they are like PE—CO_2H.

D. Patterning Ligands on Reactive SAMs

Patterning ligands on surfaces has several applications: for example, in biosensors using patterned proteins and cells, and in diagnostic tools using patterned DNA fragments, antibodies, and antigens. The techniques used for patterning ligands are often based on photolithographical procedures: these methods may be incompatible with many types of ligands.

Combination of μCP and chemical reaction on a reactive SAM presenting a mixture of active NHS ester groups and oligo(ethylene glycol) groups provides a convenient, inexpensive, and versatile method for patterning ligands on surfaces that can be recognized and bound specifically by biomacromolecules [212]. Figure 15 describes a procedure that has several steps: (i) formation of mixed SAMs presenting thiol **1** and **2**; (ii) activation by immersion in a solution of EDC (0.1 M) and pentafluorophenol (0.2 M) for 10 min; and (iii) printing a biotin-containing amine to the reactive SAMs by bringing a freshly oxidized PDMS stamp, inked with the ligand, in contact with the substrate for 5 min. The formation of patterned SAMs presenting biotin ligands was imaged by fluorescence microscopy of substrates that were incubated in a solution of fluorescently labeled antibiotin antibody (Fig. 16a). The patterns were also detected using a different approach, in which the substrate was incubated sequentially in solutions of streptavidin, biotin-conjugate protein G, fluorescently labeled goat antirabbit IgG, and imaged by fluorescence microscopy (Fig. 16b). The smallest features resolved in images obtained by these methods were squares with a 5 μm side. The high contrast between the fluorescent regions and nonfluorescent ones indicates that the PDMS stamp delivered biotin ligands to the SAM and that they were bound specifically by its binding proteins. The coupling yields were estimated using SPR to be ~75–90% of that obtained by immersion. It was also found that oxidation of the PDMS stamp prior to inking was critical for good coupling yields.

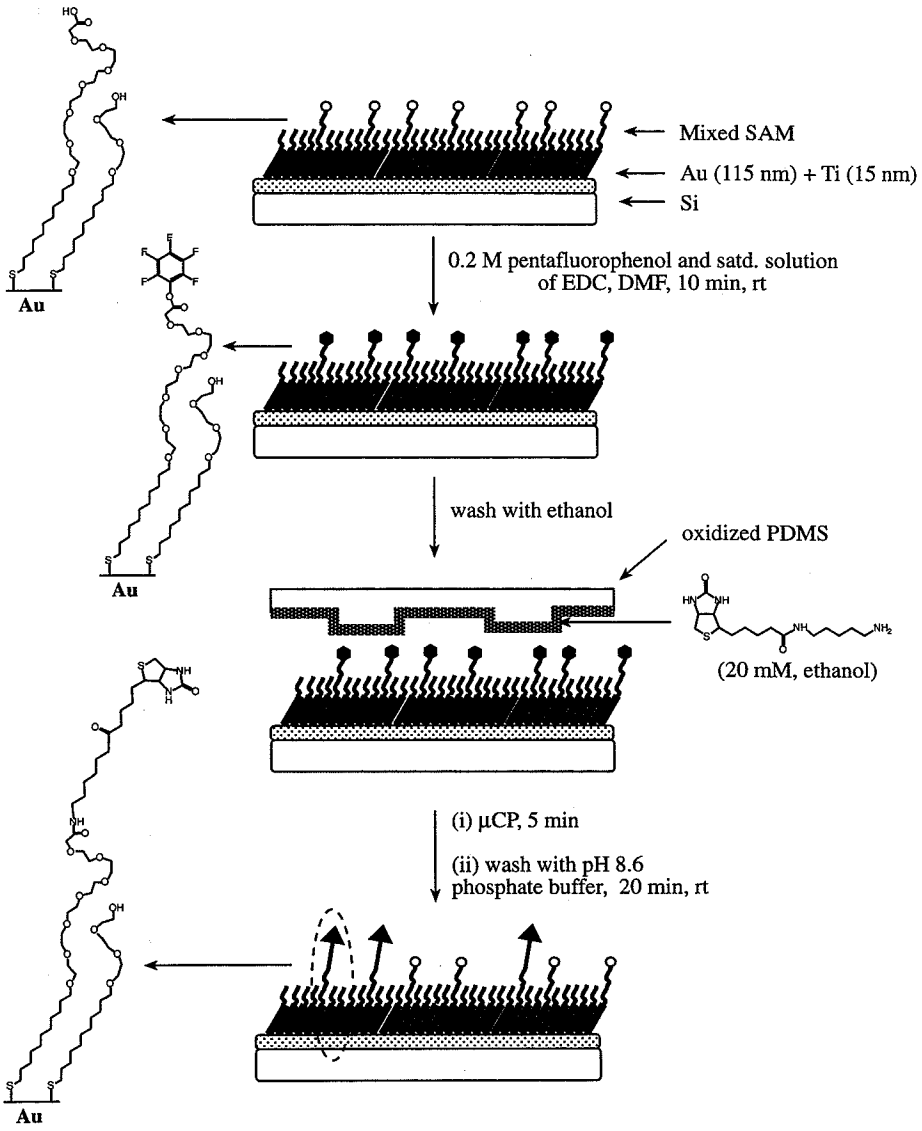

Figure 15 Schematic representation of the procedure used for patterning biotin ligands onto SAMs consisting of activated carboxylic esters. (From Ref. 212.)

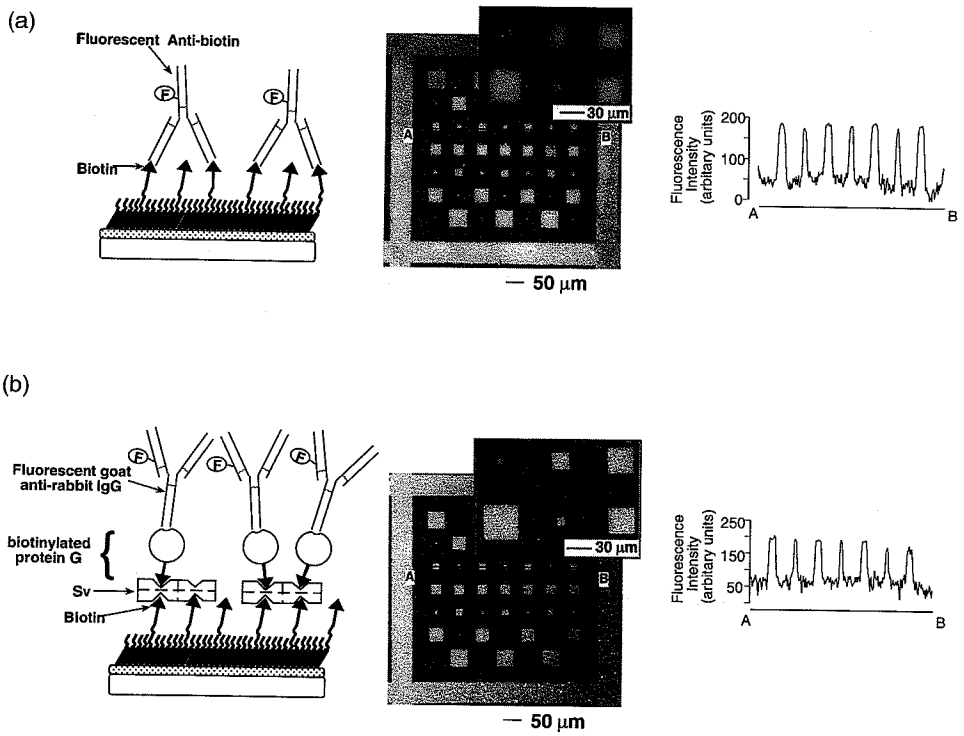

Figure 16 Fluorescence microscopy images of patterned SAMs having biotin groups (χ ~0.02) and schematic representations of the surfaces during fluorescence detection. The intensity of fluorescence in regions having biotin groups and not having ones across the line (AB) was analyzed using the NIH image software. (a) Images of fluorescently labeled antibiotin bound to patterned SAMs presenting biotin groups. (b) Images of fluorescently labeled goat anti rabbit IgG bound to SAMs presenting biotin groups that were sequentially incubated in solutions of streptavidin and biotin-conjugated protein G. (From Ref. 212.)

IX. CONCLUSIONS

SAMs can be considered as a form of insoluble, two-dimensional, and grafted polymers: that is, the substrate surface is the backbone, and the attached alkanethiolate (RS^-) groups are the sidechains. The backbone already exists before the SAM is formed: the preparation of SAMs is more like postpolymerization modification than it is like polymerization. The packing of the alkyl chains is such that the alkyl chains are highly ordered and crystallize. In SAMs of *n*-alkanethio-

lates on gold, the alkyl chains adopt an all-*trans* conformation and tilt ~30° from the normal of the substrate to maximize intermolecular interactions between adjacent chains. There is no comparable phenomenon to this tight packing of sidechains in conventional polymers. The high density of sidechains leads to anomalous reactivities of functional groups incorporated in the sidechains. SAMs provide a sterically highly congested environment. Even terminal functional groups are sterically hindered; their chemical transformations on the surface are often slower than they would be in solution. Because terminal groups are embedded in a sea of hydrophobic polymethylene chains, they are difficult to ionize. On the other hand, the high density of functional groups can result in favorable neighboring and chelating interactions.

The formation of SAMs on gold and silver is simple and convenient. The strong chemoselective interactions between the head-groups and the substrate allow SAMs to present a wide range of functional groups on the surface. Mixed and patterned SAMs deliver flexible control over the lateral distribution of chemical functionalities. Both the interchain carboxylic anhydride and the activated carboxylic esters strategy minimize the amount of orgainic synthesis required for the preparation of functionalized alkanethiols to prepare SAMs that present a wide range of chemical functionalities. They are straightforward methods and could find many applications.

ACKNOWLEDGMENTS

This work was supported by DARPA and the ONR. Lin Yan thanks Ned Bowden for technical assistance in obtaining Fig. 3.

REFERENCES

1. P Flory. Principles of Polymer Chemistry. Ithaca, NY: Cornell University Press, 1953.
2. J-M Lehn. Supramolecular Chemistry, Concepts and Perspectives. Weinheim: VCH, 1995.
3. SI Stupp, S Son, HC Lin, LS Li. Science 259:59–63, 1993.
4. H Rehage, M Veyssié. Angew Chem Int Ed Engl 29:439–448, 1990.
5. A Ulman. Introduction to Thin Organic Films: From Langmuir–Blodgett to Self-Assembly. Boston: Academic, 1991.
6. CD Bain, GM Whitesides. Angew Chem Int Ed Engl 28:506–516, 1989.
7. GM Whitesides. Chimia 44:310–311, 1990.
8. GM Whitesides, CB Gorman, eds. Self-Assembled Monolayers: Models for Organic Surface Chemistry. Handbook of Surface Imaging and Visualization. Boca Raton, FL: CRC, 1995, pp 713–733.

9. GS Ferguson, MK Chaudhury, HA Biebuyck, GM Whitesides. Macromolecules 26:5870–5875, 1993.
10. LH Dubois, RG Nuzzo. Annu Rev Phys Chem 43:437–463, 1992.
11. S Yitzchaik, T Marks. Acc Chem Res 29:197–202, 1996.
12. AR Bishop, RG Nuzzo. Curr Opin Coll Interf Sci 1:127–136, 1996.
13. A Ulman. Chem Rev 96:1533–1554, 1996.
14. RG Nuzzo, BR Zegarski, LH Dubois. J Am Chem Soc 109:733–740, 1987.
15. PE Laibinis, MA Fox, JP Folkers, GM Whitesides. Langmuir 7:3167–3173, 1991.
16. PE Laibinis, GM Whitesides. J Am Chem Soc 114:9022–9027, 1992.
17. H Lee, LJ Kepley, H-G Hong, TE Mallouk. J Am Chem Soc 110:618–620, 1988.
18. D Li, MA Ratner, TJ Marks, C Zhang, J Yang, GK Wong. J Am Chem Soc 112: 7389–7390, 1990.
19. ME Thompson. Chem Mater 6:1168–1175, 1994.
20. SMC Neiva, JAV Santos, JC Moreira, Y Gushikem, H Vargas, DW Franco. Langmuir 9:2982–2985, 1993.
21. MGL Petrucci, AK Kakkar. J Chem Soc Chem Commun 1577–1578, 1995.
22. J Sagiv. Isr J Chem 18:339–345, 1979.
23. J Sagiv. J Am Chem Soc 102:92–98, 1980.
24. I Haller. J Am Chem Soc 100:8050–8055, 1978.
25. SR Wasserman, GM Whitesides, IM Tidswell, BM Ocko, PS Pershan, JD Axe. J Am Chem Soc 111:5852–5861, 1989.
26. SR Wasserman, Y-T Tao, GM Whitesides. Langmuir 5:1074–1087, 1989.
27. T Nakagawa, K Ogawa, T Kurumizawa. Langmuir 10:525–529, 1994.
28. B Buszewski, RM Gadzata-Kopciuch, M Markuszewski, R Kaliszan. Anal Chem 69:3277–3284, 1997.
29. TR Lee, PE Laibinis, JP Folkers, GM Whitesides. Pure Appl Chem 63:821–828, 1991.
30. G Kataby, T Prozorov, Y Koltypin, H Cohen, CN Sukenik, A Ulman, A Gedanken. Langmuir 13:6151–6158, 1997.
31. KJ Stevenson, M Mitchell, HS White. J Phys Chem B 102:1235–1240, 1998.
32. CW Sheen, J-X Shi, J Martensson, AN Parikh, DL Allara. J Am Chem Soc 114: 1514–1515, 1992.
33. JF Dorsten, JE Maslar, PW Bohn. Appl Phys Lett 66:1755–1757, 1995.
34. Y Gu, Z Lin, RA Butera, VS Smentkowski, DH Waldeck. Langmuir 11:1849–1851, 1995.
35. DL Allara, RG Nuzzo. Langmuir 1:45–52, 1985.
36. HO Finklea, LR Robinson, A Blackburn, B Richter. Langmuir 2:239–244, 1986.
37. DL Allara, AN Parikh, F Rondelez. Langmuir 11:2357–2360, 1995.
38. DL Allara, RG Nuzzo. Langmuir 1:52–66, 1985.
39. PE Laibinis, JJ Hickman, MS Wrighton, GM Whitesides. Science 245:845–847, 1989.
40. Y-T Tao, GD Hietpas, DL Allara. J Am Chem Soc 118:6724–6735, 1996.
41. SH Chen, CW Frank. Langmuir 5:978–987, 1989.
42. YG Aronoff, B Chen, G Lu, C Seto, J Schwartz, SL Bernasek. J Am Chem Soc 119:259–262, 1997.
43. TJ Gardner, CD Frisbie, MS Wrighton. J Am Chem Soc 117:6927–6933, 1995.

44. JP Folkers, CB Gorman, PE Laibinis, S Buchholz, GM Whitesides, RG Nuzzo. Langmuir 11:813–824, 1995.
45. JE Chadwick, DC Myles, RL Garrell. J Am Chem Soc 115:10364–10365, 1993.
46. W Gao, L Dickinson, C Grozinger, FG Morin, L Reven. Langmuir 12:6429–6435, 1996.
47. JT Woodward, A Ulman, DK Schwartz. Langmuir 12:3626–3629, 1996.
48. L Bertilsson, K Potje-Kamloth, H-D Liess. J Phys Chem B 102:1260–1269, 1998.
49. CD Bain, HA Biebuyck, GM Whitesides. Langmuir 5:723–727, 1989.
50. JJ Hickman, PE Laibinis, DI Auerbach, C Zou, TJ Gardner, GM Whitesides, MS Wrighton. Langmuir 8:357–359, 1992.
51. K Uvdal, I Persson, B Liedberg. Langmuir 11:1252–1256, 1995.
52. HA Biebuyck, CD Bain, GM Whitesides. Langmuir 10:1825–1831, 1994.
53. AC Ontko, RJ Angelici. Langmuir 14:3071–3078, 1998.
54. MR Linford, CED Chidsey. J Am Chem Soc 115:12631–12632, 1993.
55. A Bansal, X Li, I Lauermann, NS Lewis. J Am Chem Soc 118:7225–7226, 1996.
56. JM Buriak, MJ Allen. J Am Chem Soc 120:1339–1340, 1998.
57. P DiMilla, JP Folkers, HA Biebuyck, R Harter, G Lopez, GM Whitesides. J Am Chem Soc 116:2225–2226, 1994.
58. LH Dubois, R Zegarski, RG Nuzzo. J Chem Phys 98:678–688, 1993.
59. DE Weisshaar, BD Lamp, MD Porter. J Am Chem Soc 114:5860–5862, 1992.
60. P Fenter, A Eberhardt, P Eisenberger. Science 266:1216–1218, 1994.
61. JJ Gerdy, WA Goodard. J Am Chem Soc 118:3233–3236, 1996.
62. JI Siepmann, IR McDonald. Thin Films 24:205–226, 1998.
63. T Sawaguchi, F Mizutani, I Taniguchi. Langmuir 14:3565–3569, 1998.
64. CD Bain, EB Troughton, Y-T Tao, J Evall, GM Whitesides, RG Nuzzo. J Am Chem Soc 111:321–335, 1989.
65. K Shimazu, I Yag, Y Sato, K Uosaki. Langmuir 8:1385–1387, 1992.
66. DS Karpovich, GJ Blanchard. Langmuir 10:3315, 1994.
67. TW Schneider, DA Buttry. J Am Chem Soc 115:12391, 1993.
68. Y-T Kim, RI McCarley, AJ Bard. Langmuir 9:1941, 1993.
69. W Pan, CJ Durning, NJ Turro. Langmuir 12:4469–4473, 1996.
70. RC Thomas, L Sun, RM Crooks, AJ Ricco. Langmuir 7:620, 1991.
71. TT Ehler, N Malmberg, LJ Noe. J Phys Chem B 101:1268, 1997.
72. M Buck, F Eisert, J Fischer, M Grunze, F Traeger. Appl Phys A A53:552–6, 1991.
73. RH Terrill, TA Tanzer, PW Bohn. Langmuir 14:845–854, 1998.
74. MA Bryant, JE Pemberton. J Am Chem Soc 113:8284–8293, 1991.
75. CA Widrig, C Chung, MD Porter. J Electroanal Chem 310:335–359, 1991.
76. K Hu, AJ Bard. Langmuir 14:4790–4794, 1998.
77. GE Poirier, ED Pylant. Science 272:1145–1148, 1996.
78. R Yamada, K Uosaki. Langmuir 14:855–861, 1998.
79. GE Poirier. Langmuir 15:1167–1175, 1999.
80. Y Xia, N Venkateswaran, D Qin, J Tien, GM Whitesides. Langmuir 14:363–371, 1998.
81. Z Hou, NL Abbott, P Stroeve. Langmuir 14:3287–3297, 1998.
82. A Kumar, NA Abbott, E Kim, HA Biebuyck, GM Whitesides. Acc Chem Res 28: 219–226, 1995.

83. J Tien, Y Xia, GM Whitesides. Thin Films 24:227–253, 1998.
84. RG Nuzzo, FA Fusco, DL Allara. J Am Chem Soc 109:2358–2368, 1987.
85. MD Porter, TB Bright, DL Allara, CED Chidsey. J Am Chem Soc 109:3559–3568, 1987.
86. AN Parikh, DL Allara. J Chem Phys 96:927–945, 1992.
87. RG Nuzzo, LH Dubois, DL Allara. J Am Chem Soc 112:558–569, 1990.
88. C Zubraegel, C Deuper, F Schneider, M Neumann, M Grunze, A Schertel, C Woell. Chem Phys Lett 238:308–312, 1995.
89. CA Widrig, CA Alves, MD Porter. J Am Chem Soc 113:2805–2810, 1991.
90. CA Alves, EL Smith, MD Porter. J Am Chem Soc 114:1222–1227, 1992.
91. GE Poirier, MJ Tarlov. Langmuir 10:2853–2856, 1994.
92. P Fenter, P Eisenberger. Phys Rev Lett 70:2447, 1993.
93. CED Chidsey, G-Y Liu, P Rowntree, G Scoles. J Chem Phys 91:4421–4423, 1989.
94. N Camillone III, CED Chidsey, G-Y Liu, TM Putvinski, G Scoles. J Chem Phys 94:8493–8502, 1991.
95. L Strong, GM Whitesides. Langmuir 4:546–558, 1988.
96. JJ Hickman, D Ofer, C Zou, MS Wrighton, PE Laibinis, GM Whitesides. J Am Chem Soc 113:1128–1132, 1991.
97. DM Collard, MA Fox. Langmuir 7:1192–1197, 1991.
98. CD Bain, EB Troughton, Y-T Tao, J Evall, GM Whitesides, RG Nuzzo. J Am Chem Soc 111:321–335, 1989.
99. LH Dubois, BR Zegarski, RG Nuzzo. J Am Chem Soc 112:570–579, 1990.
100. TR Lee, RI Carey, HA Biebuyck, GM Whitesides. Langmuir 10:741–749, 1994.
101. CED Chidsey, DN Loiacono. Langmuir 6:709, 1990.
102. PE Laibinis, GM Whitesides, DL Allara, Y-T Tao, AN Parikh, RG Nuzzo. J Am Chem Soc 113:7152–7167, 1991.
103. H Sellers, A Ulman, Y Shnidman, JE Eilers. J Am Chem Soc 115:9389–9401, 1993.
104. A Ulman, JE Eilers, N Tillman. Langmuir 5:1147–1152, 1989.
105. J Hautman, ML Klein. J Chem Phys 91:4994–5001, 1989.
106. J Hautman, ML Klein. J Chem Phys 93:7483–7492, 1990.
107. J Hautman, JP Bareman, W Mar, ML Klein. J Chem Soc Faraday Trans 87:2031–2037, 1991.
108. W Mar, ML Klein. Langmuir 10:188–196, 1994.
109. JI Siepmann, IR McDonald. Molec Phys 79:457–473, 1993.
110. AJ Pertsin, M Grunze. Langmuir 10:3668–3674, 1994.
111. KM Beardmore, JD Kress, N Gronbech-Jensen, AR Bishop. Chem Phys Lett 286: 40–45, 1998.
112. G Nelles, H Schonherr, M Jaschke, H Wolf, M Schaub, J Kuther, W Tremel, E Bamberg, H Ringsdorf, H-J Butt. Langmuir 14:808–815, 1998.
113. M Sprik, E Delamarche, B Michel, U Rothlisberger, ML Klein, H Wolf, H Ringsdorf. Langmuir 10:4116–4130, 1994.
114. Y-T Tao, M-T Lee, S-C Chang. J Am Chem Soc 115:9547–9555, 1993.
115. E Sabatani, J Cohen-Boulakia, M Bruening, I Rubinstein. Langmuir 9:2974–2981, 1993.

116. JM Tour, LI Jones, DL Pearson, JJS Lamba, TP Burgin, GM Whitesides, DL Allara, AN Parikh, SV Atre. J Am Chem Soc 117:9529–9534, 1995.
117. A-A Dhirani, RW Zehner, RP Hsung, P Guyot-Sionnest, LR Sita. J Am Chem Soc 118:3319–3320, 1996.
118. T-W Li, I Chao, Y-T Tao. J Phys Chem B 102:2935–2946, 1998.
119. CA Alves, MD Porter. Langmuir 9:3507–3512, 1993.
120. G-Y Liu, P Fenter, CED Chidsey, DF Ogletree, P Eisenberger, M Salmeron. J Chem Phys 101:4301–4306, 1994.
121. K Edinger, A Golzhauser, K Demota, C Woll, M Grunze. Langmuir 9:4–8, 1993.
122. C Schonenberger, JAM Sondag-Huethorst, J Jorritsma, LGJ Fokkink. Langmuir 10:611–614, 1994.
123. PG van Patten, JD Noll, ML Myrick. J Phys Chem B 101:7874–7875, 1997.
124. J Thome, M Himmelhaus, M Zharnikov, M Grunze. Langmuir 14:7435–7449, 1998.
125. M Mrksich, GM Whitesides. Ann Rev Biophys Biomol Struct 25:55–78, 1996.
126. JP Folkers, PE Laibinis, GM Whitesides. J Adhesion Sci Tech 6:1397–1410, 1992.
127. MK Chaudhury, GM Whitesides. Science 255:1230–1232, 1992.
128. GK Jennings, JC Munro, T-H Yong, PE Laibinis. Langmuir 14:6130–6139, 1998.
129. FP Zamborini, RM Crooks. Langmuir 14:3279–3286, 1998.
130. Y Xia, GM Whitesides. Angew Chem Int Ed Engl 37:550–575, 1998.
131. R Maoz, J Sagiv. Langmuir 3:1034–1044, 1987.
132. R Maoz, J Sagiv. Langmuir 3:1045–1051, 1987.
133. N Abbott, A Kumar, GM Whitesides. Chem Mater 6:596–602, 1994.
134. Y Xia, X-M Zhao, E Kim, GM Whitesides. Chem Mater 7:2332–2337, 1995.
135. MA Rampi, OJA Schueller, GM Whitesides. Appl Phys Lett 72:1781–1783, 1998.
136. KL Prime, GM Whitesides. Science 252:1164–1167, 1991.
137. KL Prime, GM Whitesides. J Am Chem Soc 115:10714–10721, 1993.
138. L Deng, M Mrksich, GM Whitesides. J Am Chem Soc 118:5136–5137, 1996.
139. CD Bain, GM Whitesides. J Am Chem Soc 110:6560–6561, 1988.
140. L Bertilsson, B Liedberg. Langmuir 9:141–149, 1993.
141. JP Folkers, PE Laibinis, GM Whitesides, J Deutch. J Phys Chem 98:563–571, 1994.
142. Y Li, J Huang, RTJ McIver, JC Hemminger. J Am Chem Soc 114:2428–2432, 1992.
143. Y Sato, R Yamada, F Mizutani, K Uosaki. Chem Lett 987–988, 1997.
144. WA Hayes, H Kim, X Yue, SS Perry, C Shannon. Langmuir 13:2511–2518, 1997.
145. DG Kurth, T Bein. Angew Chem Int Ed Engl 31:336–338, 1992.
146. DG Kurth, T Bein. Langmuir 9:2965–2973, 1993.
147. JH Moon, JW Shin, SY Kim, JW Park. Langmuir 12:4621–4624, 1996.
148. DA Hutt, GJ Leggett. Langmuir 13:2740–2748, 1997.
149. S Pan, DG Castner, BD Ratner. Langmuir 14:3545–3550, 1998.
150. H-J Himmel, K Weiss, B Jager, O Dannenberger, M Grunze, C Woll. Langmuir 13:4943–4947, 1997.
151. S Lofas, B Johnsson. J Chem Soc Chem Commun 1526–1528, 1990.
152. A Ulman, N Tillman. Langmuir 5:1418–1420, 1989.
153. RV Duevel, RM Corn. Anal Chem 64:337–342, 1992.

154. M Wells, RM Crooks. J Am Chem Soc 118:3988–3989, 1996.
155. GJ Leggett, CJ Roberts, PM Williams, MC Davies, DE Jackson, SJB Tendler. Langmuir 9:2356–2362, 1993.
156. J Wang, JR Kenseth, VW Hones, J-B Green, MT McDermott, MD Porter. J Am Chem Soc 119:12796–12799, 1997.
157. YW Lee, J Reed-Mundell, CN Sukenik, JE Zull. Langmuir 9:3009–3014, 1993.
158. SM Amador, JM Pachence, R Fischetti, JPJ McCauley, ABI Smith, JK Blasie. Langmuir 9:812–817, 1993.
159. P Kohli, KK Taylor, JJ Harris, GJ Blanchard. J Am Chem Soc 120:11962–11968, 1998.
160. N Tillman, A Ulman, JF Elman. Langmuir 5:1020–1026, 1989.
161. RCJ Horton, TM Herne, DC Myles. J Am Chem Soc 119:12980–12981, 1997.
162. N Balachander, CN Sukenik. Langmuir 6:1621–1627, 1990.
163. TS Koloski, CS Dulcey, QJ Haralson, JM Calvert. Langmuir 10:3122–3133, 1994.
164. GE Fryxell, PC Rieke, LL Wood, MH Engelhard, RE Williford, GL Graff, AA Campbell, RJ Wiacek, L Lee, A Halverson. Langmuir 12:5064–5075, 1996.
165. A Benninghoven, B Hagenhoff, E Niehuis. Anal Chem 65:630A–640A, 1993.
166. S Akari, D Horn, H Keller, W Schrepp. Adv Mater 7:549–551, 1995.
167. L Yan, C Marzolin, A Terfort, GM Whitesides. Langmuir 13:6704–6712, 1997.
168. RG Cooks. Chem Ind 142, 1955.
169. L Yan, X-M Zhao, GM Whitesides. J Am Chem Soc 120:6179–6180, 1998.
170. J Rao, L Yan, B Xu, GM Whitesides. J Am Chem Soc 121:2629–2630, 1999.
171. L Yan, WTS Huck, X-M Zhao, GM Whitesides. Langmuir 15:1208–1214, 1999.
172. J Lahiri, L Isaacs, J Tien, GM Whitesides. Anal Chem 71:777–790, 1999.
173. HA Biebuyck, GM Whitesides. Langmuir 10:4581–4587, 1994.
174. NB Larsen, H Biebuyck, E Delamarche, B Michel. J Am Chem Soc 119:3017–3026, 1997.
175. Y Xia, D Qin, GM Whitesides. Adv Mater 8:1015–1017, 1996.
176. R Jackman, J Wilbur, GM Whitesides. Science 269:664–666, 1995.
177. Y Xia, M Mrksich, E Kim, GM Whitesides. J Am Chem Soc 117:9576–9577, 1995.
178. NL Jeon, K Finnie, K Branshaw, RG Nuzzo. Langmuir 13:3382–3391, 1997.
179. PC Hidber, W Helbig, E Kim, GM Whitesides. Langmuir 12:1375–1380, 1996.
180. PC Hidber, PF Nealey, W Helbig, GM Whitesides. Langmuir 12:5209–5215, 1996.
181. A Bernard, E Delamarche, H Schmid, B Michel, HR Bosshard, H Biebuyck. Langmuir 14:2225–2229, 1998.
182. CD James, RC Davis, L Kam, HG Craighead, M Isaacson, JN Turner, W Shain. Langmuir 14:741–744, 1998.
183. GM Whitesides, PE Laibinis. Langmuir 6:87–96, 1990.
184. KR Stewart, GM Whitesides, HP Godfried, IF Silvera. Rev Sci Instr 57:1381–1383, 1986.
185. M Mrksich, GM Whitesides, ed. Using Self-Assembled Monolayers That Present Oligo(ethylene glycol) Groups to Control the Interactions of Proteins with Surfaces. Poly(ethylene glycol) Chemistry and Biological Applications, vol. 680. Washington, DC: American Chemical Society, 1997, pp 361–373.

186. M Nishizawa, M Shibuya, T Sawaguchi, T Matsue, I Uchida. J Phys Chem 95: 9042–9044, 1991.
187. PL Burn, A Kraft, DR Baigent, DDC Bradley, AR Brown, RH Friend, RW Gymer, AB Holmes, RW Jackson. J Am Chem Soc 115:10117–10124, 1993.
188. L Dai, IIJ Griesser, X IIong, AWII Mau, TII Spurling, Y Yang, JW White. Macromolecules 29:282–287, 1996.
189. PL Burn, AB Holmes, A Kraft, DDC Bradley, AR Brown, RH Friend, RW Gymer. Nature 356:47–49, 1992.
190. BG Healey, SE Foran, DR Walt. Science 269:1078–1080, 1995.
191. W Knoll, M Matsuzawa, A Offenhausser, J Ruhe. Isr J Chem 36:357–369, 1996.
192. Y Liu, M Zhao, DE Bergbreiter, RM Crooks. J Am Chem Soc 119:8720–8721, 1997.
193. R Langer, JP Vacanti. Science 260:920–926, 1993.
194. SA Sukhishvili, S Granick. Langmuir 13:4935–4938, 1997.
195. Y Liu, ML Bruening, DE Bergbreiter, RM Crooks. Angew Chem Int Ed Engl 36: 2114–2116, 1997.
196. G Decher. Science 277:1232–1237, 1997.
197. PT Hammond, GM Whitesides. Macromolecules 28:7569–7571, 1995.
198. JM Stouffer, TJ McCarthy. Macromolecules 21:1204–1208, 1988.
199. TJ Lenk, VM Hallmark, JF Rabolt, L Haussling, H Ringsdorf. Macromolecules 26:1230–1237, 1993.
200. L Rozsnyai, MS Wrighton. J Am Chem Soc 116:5993–5994, 1994.
201. G Mao, DG Castner, DW Grainger. Chem Mater 9:1741–1750, 1997.
202. SL Clark, MF Montague, PT Hammond. Macromolecules 30:7237–7244, 1997.
203. E Kim, GM Whitesides, LK Lee, SP Smith, M Prentiss. Adv Mater 8:139–142, 1996.
204. A Karim, JF Douglas, BP Lee, SC Glotzer, JA Rogers, RJ Jackman, EJ Aims, GM Whitesides. Phys Rev E: Stat Phys, Plasmas, Fluids, Relat Interdiscip Top 57: R6273–R6276, 1998.
205. M Boltau, S Walheim, M Jurgen, G Krausch, U Steiner. Nature 391:877–879, 1998.
206. S Zhang, L Yan, M Altman, M Lässle, H Nugent, F Frankel, DA Lauffenburger, GM Whitesides, A Rich. Biomaterials 20:1213–1220, 1999.
207. SR Holmes-Farley, RH Reamey, TJ McCarthy, J Deutch, GM Whitesides. Langmuir 1:725–740, 1985.
208. SR Holmes-Farley, GM Whitesides. Langmuir 2:62–76, 1986.
209. SR Holmes-Farley, C Bain, GM Whitesides. Langmuir 4:921–937, 1988.
210. CD Bain, GM Whitesides. J Am Chem Soc 111:7164–7175, 1989.
211. CD Bain, GM Whitesides. Langmuir 5:1370–1378, 1989.
212. J Lahiri, E Ostuni, GM Whitesides. Langmuir 15:2055–2060, 1999.